Int J Mater Form (2015) 8:183–196
DOI 10.1007/s12289-013-1159-2

ORIGINAL RESEARCH

Micro-punching of aluminum foil by laser dynamic flexible punching process

Huixia Liu · Mengmeng Lu · Xiao Wang · Zongbao Shen · Chunxing Gu · Yuxuan Gu

Received: 11 September 2013 / Accepted: 27 November 2013 / Published online: 17 December 2013
© Springer-Verlag France 2013

Abstract A novel microscale laser dynamic flexible punching technology combining flexible punching and laser shock forming is presented. The ultrahigh strain rates of workpiece's material and soft punch driven by dynamic shock load are the significant feature of this process. In the present study, arrays of 300 μm×300 μm square holes with good sheared edges quality are obtained on 20 μm Al foils. The shearing behavior is also investigated through investigating cross section of punched hole. As a piece of polyurethane rubber loaded by the ultra-high transient pressure of laser supported detonation wave (LSD) is employed as soft punch, the new process has such advantages as homogenizing pressure, easy demould and reducing springback. To study more details in an extremely short interval, simulations are conducted by ANSYS/LS-DYNA and LS-PrePost. The methods of Finite Element Mesh (FEM) and Smoothed Particle Hydrodynamics (SPH) are used. The relationship between soft punch thickness and corresponding minimum punching energy for various workpiece thicknesses is revealed. In addition, the material flowing behavior around the sheared edges has also been discussed. The results in this paper indicate that the present process is promising to fabricate high quality micro holes in the micro scale application.

Keywords Microscale laser dynamic flexible punching · Soft punch · Process simulations · Smoothed particle hydrodynamics (SPH) · Material flowing

H. Liu (✉) · M. Lu · X. Wang · Z. Shen · C. Gu · Y. Gu
School of Mechanical Engineering, Jiangsu University, Zhenjiang 212013, China
e-mail: lhx@ujs.edu.cn

Introduction

Micro-punching [1] which can be traced back to the latter part of the last century is not a new topic in the field of micro metal forming. However, it is still a micro-manufacturing process with enormous potentiality due to the simplicity of the process, low cost, high production capability and accuracy [2]. For instance, it is a suitable method to fabricate some types of chip lead frames used in IT industry [3]. About this process, there are several existing visions. Masuzawa et al. [4] first proposed a micro-punching process with the micro-die fabricated by micro-EDM. Chern et al. [5] presented a micro-punching apparatus to fabricate micro micro-punch and then micro-die within the same machine, completely eliminating the eccentricity between the punch and the die. Qin et al. [6] reported the development of a prototype micro-sheet-forming machine system. Santo et al. [7] proposed a miniaturized forming machine which was consisted of piezo-electric actuator and a small load cell assembled in the same frame. The punch position and speed were precisely controlled and forming force could be measured. Xu et al. [8] carried out a micro-punching process of brass foil by using a novel micro-forming system with high speed and high precision automatic drive apparatus. According to above processes, micro-holes can be punched successfully. However, the fabrication of ultra-small rigid punch and the alignment between a punch and a die are still difficult [9]. Moreover, the micro punch would be worn progressively, thus affecting the punching quality [10]. To solve these problems, a method using a flexible punch instead of a metal one has been proposed. Watari et al. [11] carried out an experimental approach to ascertain the effectiveness of a flexible punching method using a urethane elastomer for SUS304 sheets of 50 and 100 μm in thickness, single circular holes of 1~5 mm in diameter were punched. Rhim

et al. [12] proposed a method by which multiple holes of ultra small size about 2~10 μm can be punched simultaneously.

Recently, the rapid development of laser shock forming(LSF) technology provides a new approach to manufacture microparts [13]. The laser beam is more localized and its pulse energy can be much more precisely-controlled, thus it can realize local forming for parts even having complex shapes. Liu et al. [14] proposed a novel micro scale laser high speed punching process in which a 10 μm metal sheet with a sacrificial coating was impacted directly by a short and intense laser pulse. Liu et al. [15] also investigated the micro-punching process by laser-driven flyer and micro holes of about 800 μm in diameter were punched on the 10 μm copper foil.

In view of the fact that the flexible punching and laser shock forming have advantages given above, this paper presents a novel microscale laser dynamic flexible punching process which couples two effective processes as a new micro-punching process. The ultrahigh strain rates of workpiece's material and the soft punch driven by shock load are the significant features in this process. A piece of thin polyurethane rubber is utilized as soft punch to load the thin metal sheet. Using the soft punch as the pressure medium has lots of advantages:

Firstly, the soft punch can protect the thin metal sheet from being ablated when ablative layer is directly applied to the surface of the workpiece;

Secondly, the soft punch is more suitable for punching micro holes with ultra small size and complex shape for the flexible rubber's high level of resolution in the sub-micron ranges [12].

Thirdly, allowing for the hyperelastic characteristic of rubber, it will be very easy to draw out the soft punch from the punched holes in thin metal sheet quickly, namely the demould process is easy.

In the present study, arrays of square holes of 300 μm×300 μm in size are punched on 20 μm Al foils by using a soft punch, under the impact of the single pulse laser. The shearing behavior of the process is also investigated with cross section of punched hole. Meanwhile, a series of simulations which study the details in different periods are given. The simulations are conducted based on methods of Finite Element Mesh (FEM) and Smoothed Particle Hydrodynamics (SPH). The Fabbro model is used to simulate the laser induced plasma shock wave pressure. The Johnson-Cook model is adopted to describe the material behavior of workpiece within an ultrahigh strain rate range. The Mooney-Rivlin model is used to describe the hyperelastic flexible rubber materials' deformation behavior in dynamic analysis.

Process design and experiment

Laser dynamic flexible punching

Figure 1 shows the basic concept of the present microscale laser dynamic flexible punching process schematically. The experimental apparatus mainly consists of pressing block, confinement layer, ablative layer, soft punch, workpiece, punching die and 3D mobile platform. At the very beginning, an intense laser pulse irradiates onto the ablative layer. The material of ablative layer is vaporized into a high-temperature and high-pressure plasma instantaneously after absorbing large amounts of laser energy. In the confined ablation mode, the plasma expansion occurring in a limited space causes a laser supported detonation wave (LSD). Then the induced shock wave propagates into the soft punch very soon. As the flexible rubber material has the incompressible and hyperelastic characteristics, the workpiece will be loaded by the soft punch in the next moment. Due to the constraint of punching die, shear stress develops in the target section of the workpiece. Eventually, the punching is realized. Meanwhile, the soft punch is drawn into the die-opening cavities after passing through the punched holes. However, it can spring back in hundreds of nanoseconds and finally restores its flatness. Thus demould is fairly easy.

Experiment device and preparation

Hardened and tempered AISI 1095 high-carbon steel is used as punching die material due to its high stiffness and high hardness. The chemical compositions and mechanical properties are listed in Table 1. The sheet used to make punching die is 0.5 mm in thickness and the through die-openings in the center position are fabricated by picosecond laser. Figure 2 shows the full view of the punching die observed under the KEYENCE VHX-1000C digital microscope with a depth-of-field and resolution that are unmatched by conventional optical microscopes. Four square holes of 300 μm×300 μm in size are evenly distributed in a box of 2 mm×2 mm in size. After the polishing treatment, the punching die has good surface quality. The edges of die-openings are sharp enough due to the ultra small resolution of picosecond laser. In the process, the punching die is fixed on a 3D mobile platform, thus the alignment of die center and laser spot can be achieved quickly.

Al foil of 20 μm in thickness is selected because it is commonly used for MEMS applications. The commercially available Al foils are cut into10mm×10 mm workpieces. Then, the thin metal workpiece is placed on the top of the punching die, just covering the total die-openings completely.

Polyurethane rubber with the Shore A hardness 70° is employed to make the soft punches. The rubber thickness selected in the process are 100 μm,200 μm and 300 μm. Like workpieces, they are also cut into square pieces of 10 mm×

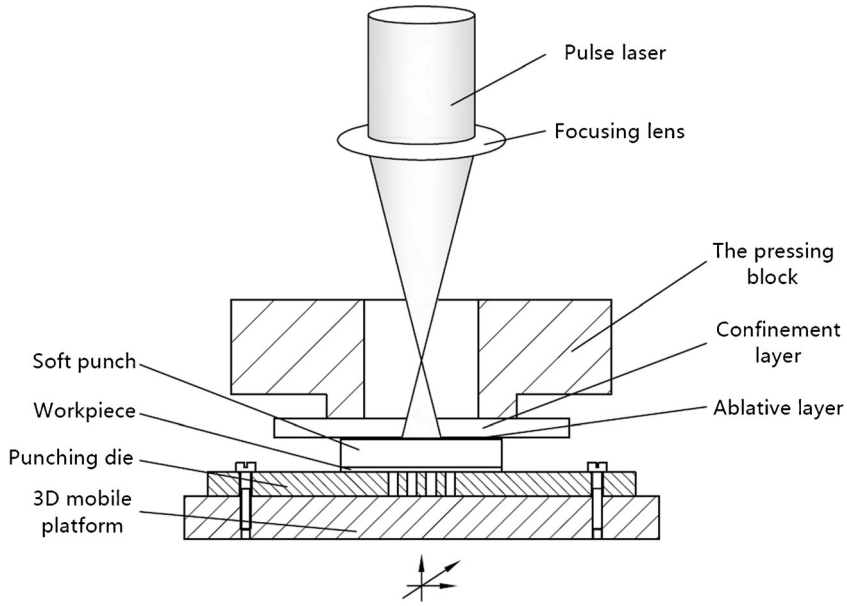

Fig. 1 Schematic diagram of microscale laser dynamic flexible punching

10 mm. A black paint coating working as ablative layer, on the supper surface of soft punch, can well protect the soft punch and greatly enhance the absorption rate of the pulse laser energy. Then, the soft punch is adhered onto the center position of K9 glass confinement layer, water as a good binder. A heavy flange used as pressing block plays a considerable role in providing the preloaded force. Thus contact surfaces can be packed tightly with each other and plasma leak can be prevented at the interface of confinement layer and ablative layer.

In the study, a short pulse Nd-YAG laser (INNOLAS Spitlight 2000) with Gaussian distribution beam is employed. The laser's main parameters associated with the experiments are listed in following Table 2.

In order to get the anticipant laser spot to cover the impact zone completely, an appropriate defocusing is necessary. When the focus is above the workpiece, the value of defocusing is defined as positive. In this study, the defocusing is set to 30 mm, and the corresponding spot diameter is 2.5 mm.

Experimental results and discussions

Arrays of square holes are punched successfully on thin Al foils with laser dynamic flexible punch. The geometrical accuracy of punched holes is examined with the KEYENCE VHX-1000C digital microscope, and the shearing behavior is also investigated by surveying cross section of holes. It is shown, in Fig. 3a, that a piece of Al foil is completely punched with four square holes. And Fig. 3b shows the enlarged view of one accurately reproduced square hole. It can be found that dimensional accuracy and sheared edge quality are excellent.

To investigate hole quality, the punched hole is sectioned as shown in Fig. 4a. The corresponding partial enlarged view is shown in Fig. 4b. In addition, the characteristic profile of punched holes such as rollover, burnish, fracture, and burr are defined as shown in Fig. 4c. The results are analyzed considering the well-known shape of mechanically punched holes [16]. Compared with the section profile of holes punched in static load condition, which is carried out by Joo et al. [9], it can be found that the punched holes punched in dynamic shock load condition have the sheared edge profile with large rollover depth, small burnish depth, rather small fracture depth and small tapering angle.

A reasonable explanation can be given for the difference in terms of stress wave theory, namely, the yield stress and strength limit increase greatly under the dynamic shock load and the phenomena of delayed yield and delayed fracture are even more evident. And, as the punching is a novel process with no punching clearance between soft punch and die-opening, the tapering angle in the sheared edge profile should

Table 1 Chemical compositions and mechanical properties of punching die material

Material	Chemical composition						Mechanical properties		
	C wc %	Si wc %	Mn wc %	P wc %	S wc %	Cr wc %	Hardness HRC	Tensile strength(MPa)	Shear modulus(Gpa)
AISI 1095	≤1.05	0.15–0.30	0.30–0.45	≤0.02	≤0.02	0.01	58	1600–1800	80

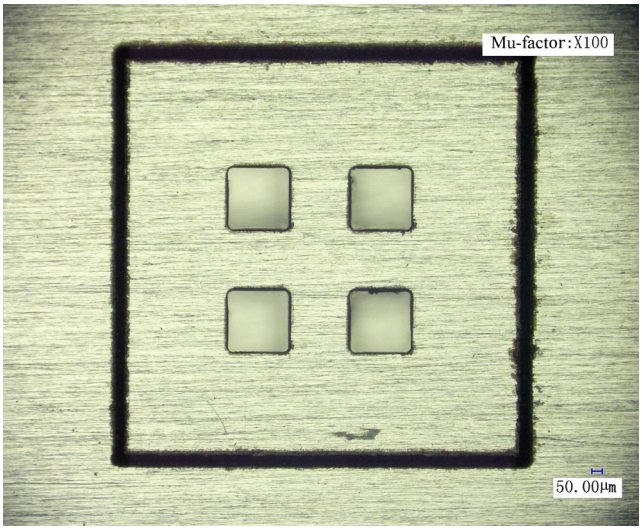

Fig. 2 The punching die used in the present study

be rather small. Generally, a burr cannot be developed in cast iron due to fracture in the initial stage [17]. However, some burrs can be found in the sheared edge profile of the present punching, this is because of the effect of good ductility of Al.

In this process, the optical energy of the laser beam has been turned into mechanical energy of the shock wave. The soft punch acts on the thin metal sheet without any overheating, thus the micro-punching is a purely mechanical process. The so called material impedance mismatch effect at the interface of soft punch and thin workpiece increases the loading pressure greatly [18]. The ablative layer made of black paint is thought to greatly enhance the absorption rate of the pulse laser energy, thus improving the efficiency of energy conversion. The laser energy values set in this process are 1380 mJ, 1690 mJ and 1900 mJ. When a soft punch of 100 μm in thickness is employed, the punching effect is just appearing with 1380 mJ laser energy, and a most punching can be obtained with 1690 mJ laser energy. Along with the increasing of soft punch's thickness, more laser energy is required. When the laser energy is set to 1900 mJ, the workpiece can be punched well with the soft punch of 100 μm (Fig. 5a) and 200 μm (Fig. 5b) in thickness, but can hardly be punched by using a soft punch of 300 μm in thickness (Fig. 5c). And, the results of punching, when the 300 μm thick soft punch is used, are slightly unstable. Thus the thickness of soft punch should be selected appropriately, and the proposed value is ranging from 100 μm to 200 μm.

Considering that some blanking parts may be lodged in die-openings, an ultrasonic cleaner has played a good role to take these micro parts out.

Numerical simulation

In this study, numerical simulations are conducted by using ANSYS/LS-DYNA and LS-PrePost. The methods of Finite Element Mesh (FEM) and Smoothed Particle Hydrodynamics (SPH) are employed. Since the model as well as the pulse pressure load is completely symmetrical about planes, only a quarter of the model is established for improving computation efficiency.

Model setting

Figure 6 shows the structure of the simplified geometric model for the microscale laser dynamic flexible punching. As the model is made to simulate a purely mechanical process, the ablative layer which is used to turn optical energy into mechanical energy is certainly taken away. The pressure is directly loaded on the upper surface of the soft punch. In the experiment, the confinement layer can magnify the shock pressure by preventing the plasma from leaking out and confines the polyurethane rubber' upward deformation. However, in this simulation, the only function of confinement layer is to constrain the soft punch. Besides, simulations are carried out with two types of die models. One die model (Fig. 7a) with 2×2 array of square die-openings keeps the same size with the real object. The other model (Fig. 7b) contains 24 square die-openings distributed regularly. Each sketch located in the right side respectively shows the geometric dimensions in detail, and the loading zone is marked by some+signs. The values of workpiece thickness are selected as 10 μm, 20 μm, 30 μm, and 40 μm. Meanwhile, the soft punches are in thickness of 100 μm,200 μm,300 μm and 400 μm.

The element type Solid 164 is used for the 3D modeling of confinement layer and soft punch, which is defined by 8 nodes and used in explicit dynamic analysis only. Both Shell 163 elements and SPH particles are used for the modeling of thin

Table 2 The laser's main parameters associated with experiments

Wavelength(nm)	Pulse energy(mJ)	Pulse width(ns)	Energy stability(%)	Lens' focal length(mm)
1064	80~2000	8	<±1	100

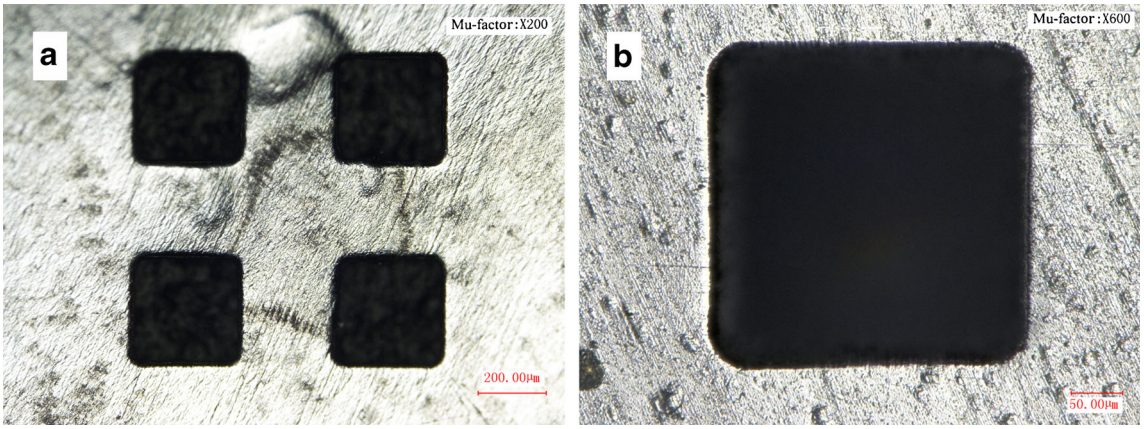

Fig. 3 Experimental results: **a** A fully punched workpiece; **b** An accurately reproduced square hole

metal workpiece. Shell163 is a 4-node element with bending and membrane capabilities. Both in-plane and normal loads are permitted. This element type is utilized in the FEM (Finite Element Method) method, while SPH particles are used in the SPH (Smooth Particle Hydrodynamics) method. SPH is a meshfree method which was developed to avoid the limitations of mesh tangling encountered in extreme deformation problems with FEM [19]. Thus, it has advantages in describing the complex material behavior under a high strain rate in the microscale laser dynamic flexible punching process. In addition, the element type Shell 163 is also used for the modeling of punching die.

Constitutive models and failure damage model

To simulate the process of microscale laser dynamic flexible punching, three different material models are used, namely the strain sensitive plasticity model for thin metal workpiece, the hyperelastic model for soft punch, and the rigid model for confinement layer and

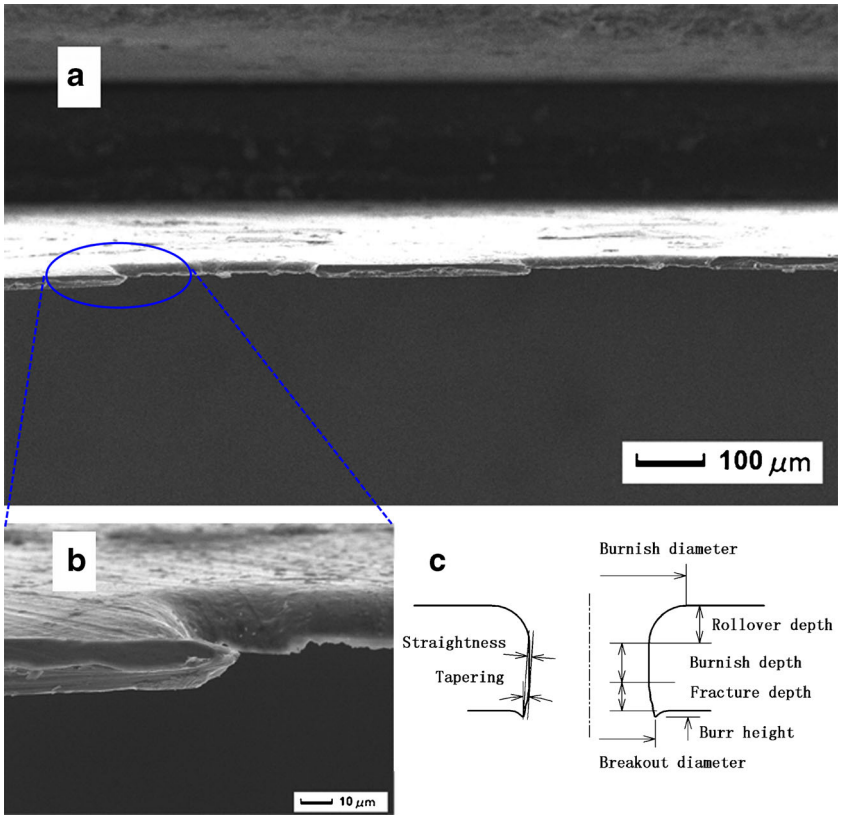

Fig. 4 Cross section of a punched hole observed by SEM: **a** The cross section; **b** The corresponding partial enlarged view; **c** The characteristic profile obtained in dynamic load condition

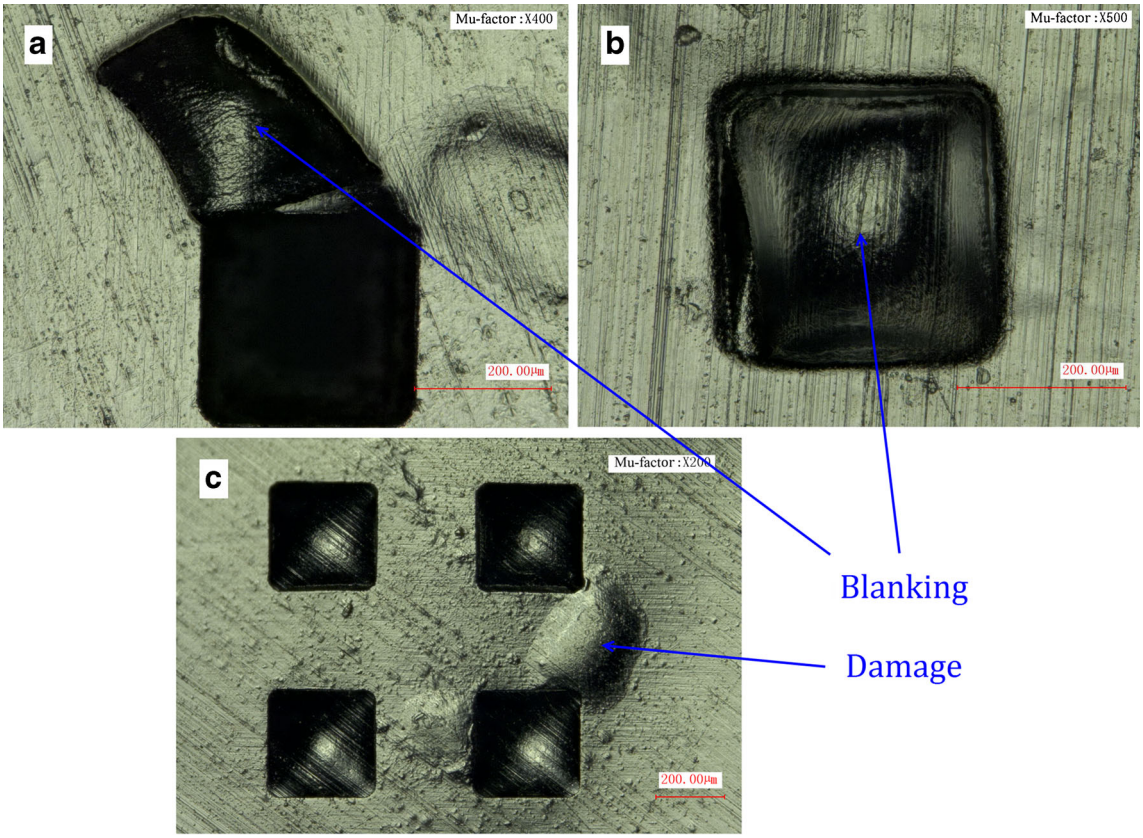

Fig. 5 Different results of micro-punching with soft punches in various thicknesses, when laser energy is set to1900mJ: **a** A fully punched hole obtained by using a 100 μm thick soft punch; **b** A punched hole obtained by using 200 μm thick soft punch; **c** Holes can hardly be punched by using a 300 μm thick soft punch

punching die. In order to obtain accurate results, precise material properties are given.

Johnson Cook model is a widely used constitutive model for materials subjected to large strains and high strain rate [20]. When the thin metal sheet is punched within hundreds of nanoseconds, with the strain rate scaling up to 10^6 to 10^7 per second, the Johnson Cook model is suitable. The simplified Johnson Cook model can be expressed as

$$\sigma = (A + B\varepsilon^n)\left(1 + C\ln\left(\frac{\dot{\varepsilon}}{\dot{\varepsilon}_0}\right)\right) \quad (1)$$

Where σ is the equivalent yield strength, ε is the equivalent plastic strain, $\dot{\varepsilon}$ is the equivalent plastic strain rate, $\dot{\varepsilon}_0$ is the reference strain rate. A, B, C and n are the material constants. Table 3 gives correlative model parameters of 2024-T 3 Aluminum.

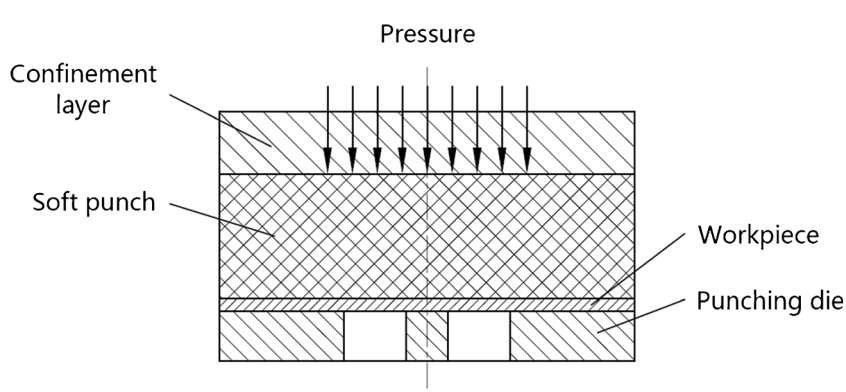

Fig. 6 Schematic of the simplified geometric model for the microscale laser dynamic flexible punching

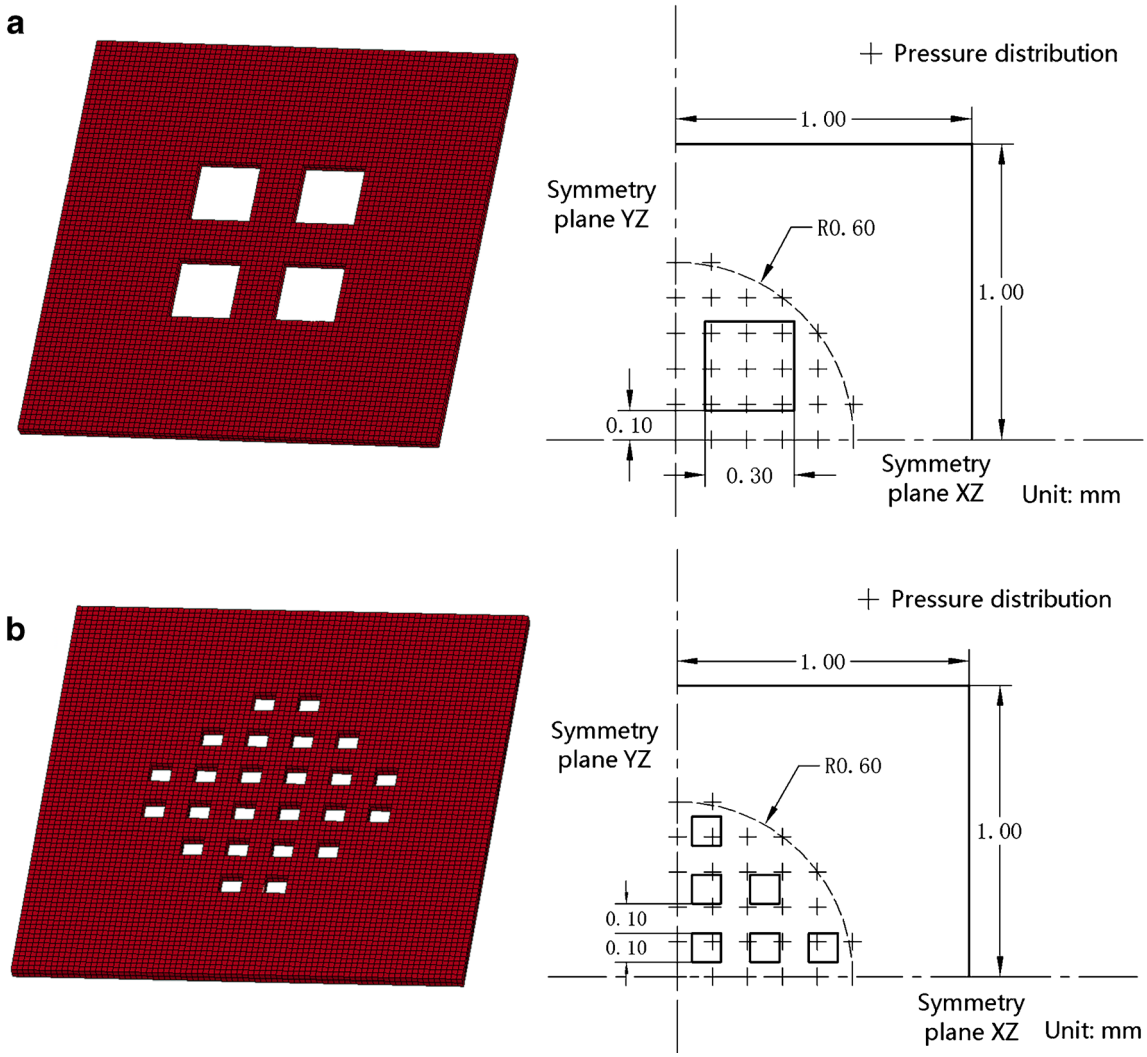

Fig. 7 Two types of die models: **a** A die model with a 2×2 array of square holes, which keeps the same size with real object; **b** The other punching die model with 24 square holes distributed regularly; Each sketch located in the *right side* shows the geometric dimensions and the loading zone which is marked by some+signs

The Johnson Cook failure criterion [21] is used as the damage initiation criteria in this process, since it takes into account the nucleation growth and coalescence of voids in ductile material at high strain rates. The strain at fracture is given by

$$\varepsilon_f = \left[d_1 + d_2 \exp\left(d_3 \frac{p}{q}\right)\right]\left[1 + d_4 \ln\left(\frac{\dot{\varepsilon}}{\dot{\varepsilon}_0}\right)\right]\left(1 + d_5 \widehat{\theta}\right) \quad (2)$$

Where ε_f is the strain at fracture, d_{1-5} are the failure parameters, $\dot{\varepsilon}_0$ is the reference strain rate, $\widehat{\theta}$ is the homologous temperature, and p/q is the ratio of pressure divided by effective stress. The correlative parameters of 2024-T 3 Aluminum used in the Johnson Cook failure mode are given in Table 4 [22].

The flexible polyurethane rubber used as soft punch has nonlinear stress–strain characteristics for enormous deformations. And in simulations, it is usually assumed as nearly

Table 3 Constitutive model parameters of 2024-T 3 aluminum

Material	A(MPa)	B(MPa)	C	n	m	$\dot{\varepsilon}_o$ (s^{-1})
2024-T 3 aluminum	369	684	0.0083	0.73	1.7	1.0

Table 4 Failure damage mode parameters of 2024-T 3 aluminum

Material	D_1	D_2	D_3	D_4	D_5
2024-T 3 aluminum	0.112	0.123	1.500	0.007	0.000

incompressible. For these causes, Mooney-Rivlin model is selected to describe the flexible rubber material's behavior [23]. It uses a strain energy function W, whose derivative with respect to a strain component determines the corresponding stress component. The form of the Mooney-Rivlin strain energy potential is shown in the following functions.

$$W = \sum_{k+m=1}^{n} C_{km}(I_1-3)^k + (I_2-3)^m + \frac{1}{2}k(I_3-1)^2 \quad (3)$$

$$\sigma_{ij} = \frac{\partial W}{\partial \varepsilon_{ij}} \quad (4)$$

In the above equations, W is the strain energy per unit of reference volume, I_1–I_3 are the strain invariants, k is the bulk modulus. Since the rubber material is assumed as incompressible, the value of I_3 is set as 1. C_{km} is the hyperelastic constant, which determines the material response. Generally, two parameters (C_{10} and C_{01}) are used to describe hyperelastic rubber deformation. And, the mechanical properties of the polyurethane rubber are given in Table 5.

Loading

The pressure is directly loaded on the upper surface of soft punch according to a simplified model shown in Fig. 6. A one-dimensional model established by Fabbro et al. [24] can be used to figure out the shock wave pressure, assuming that laser irradiation is uniform. The Fabbro model is shown as:

$$p_{\max} = 0.01 \times \left(\frac{\alpha}{2\alpha+3}\right)^{\frac{1}{2}} \times Z^{\frac{1}{2}} \times I_0^{\frac{1}{2}} \quad (5)$$

In the above equation, $P_{\max}$ is the peak pressure, α is a constant usually set as 0.1, Z is the combination impedance, which is defined by the relation

$$\frac{2}{Z} = \frac{1}{Z_1} + \frac{1}{Z_2} \quad (6)$$

Z_1 is the confinement layer's acoustic impedance, and Z_2 is the soft punch's acoustic impedance (The black paint as ablative layer is ablated by the laser beam). I_0 is the laser power density. The pressure value calculated by this 1D model is proved to be a little greater than actual value [18].

Due to the confined ablation mode, the loading time of shock wave pressure can be lengthened to three to five times of the laser pulse duration [25]. In these simulations, loading time is set to 24 ns, namely, three times of the laser pulse duration. A Pressure–time curve given in Fig. 8 indicates the law of shock wave pressure changing with time.

Table 5 Mechanical properties of the flexible rubber material

Material	Hardness shore A (°)	M-R constant C_{10} (MPa)	M-R constant C_{01} (MPa)	Poisson's ratio (μ)
Polyurethane	70	0.736	0.184	0.49997

Simulation results and discussions

Verify the reliability of the simulation

To verify the reliability of the simulation, the main conditions keep the same with the actual: the die model with die-openings of 300 μm×300 μm in size, the 20 μm thick workpiece, the soft punches with various thickness, namely, 100 μm, 200 μm, 300 μm.

Analogous to the minimum punching power in the conventional punching process, the minimum punching energy is defined as the low limit of laser energy by which a partial punching (Fig. 9b) can be obtained. Table 6 shows the comparison of the values of minimum punching energy in experiments and simulations. It turns out that the minimum punching energy of the laser pulse in simulations is lower than actual in experiments. And, the error rates remain around 10 %. This is because the value of shock wave pressure calculated by the Fabbro model is greater than the real one. Thus, adjusting with some offset for the pressure, the results of simulation are regarded as reliable.

In order to study more details that can't be captured in experiments and make up for the lack of experimental conditions, more simulations with multilevel parameters are

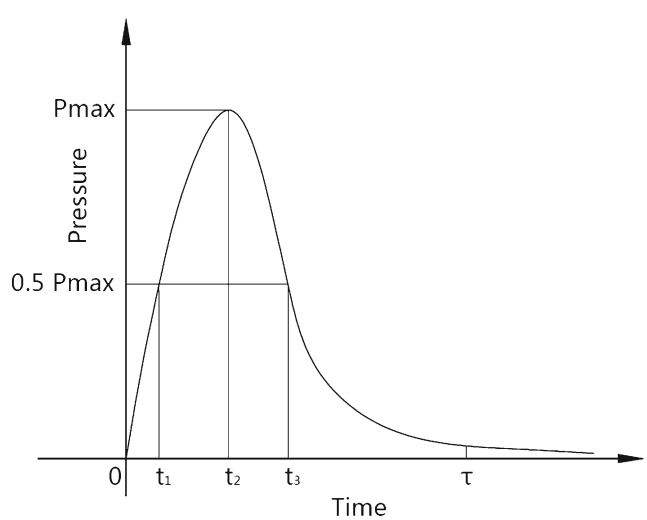

Fig. 8 The Pressure–time curve

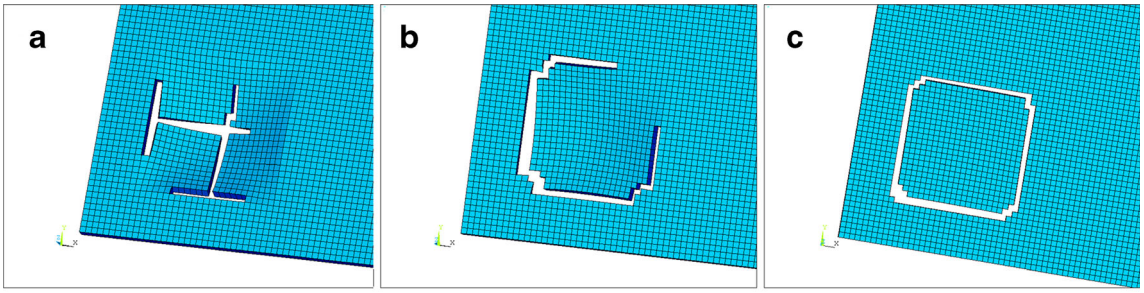

Fig. 9 Three different results in FEM simulations: **a** Abortive punching, **b** Partial punching, **c** Full punching

conducted. The relationship between the soft punch thickness and corresponding minimum punching energy for various workpiece thicknesses is revealed in Fig. 10. It can be found that the workpiece thickness has a significant influence on the minimum punching energy. However, the influence of soft punch thickness is not very notable. When the workpiece is too thick or the laser energy is too small, the effect of punching is quite different: the punching duration prolongs and the flowing of rubber material is impeded, thus stress concentration and first cracks take place in the center region of the blanking, which is shown in Fig. 9a. Then the fracture surfaces will have a poor quality. The soft punch is the key part in the microscale laser dynamic flexible punching process. It has more advantages over a rigid one. One of these advantages is that the soft punch has the ability to homogenize pressure. When the soft punch is too thin (<100 μm), the ability is reduced greatly, the punching will be unstable and blanking parts are tattered. However, when it is too thick (>300 μm), it will be more like a bulging process rather than a punching process. Therefore, an appropriate value of laser pulse energy to soft punch thickness is necessary.

Effect of dynamic deformation of soft punch

More details of punching process are investigated by using two types of die models (Fig. 7). As the laser-driven soft punch rather than a rigid punch is employed as pressure medium, its dynamic deformation has a significant effect on the punching of metal foils.

Table 6 The comparison of the minimum punching energy (Workpiece thickness: 20 μm)

NO.	Soft punch thickness (μm)	Experimental data A (mJ)	Simulative data A' (mJ)	Error rate 1-A'/A
1	100	1610	1463	9.1 %
2	200	1690	1519	10.1 %
3	300	1800	1629	9.5 %

In the first 270 ns, the induced shock wave propagates in the soft punch with a high speed. At the beginning, a transient pressure is loaded on the upper surface of soft punch and the diameter of the circular impact zone is 1.2 mm. Along with the generation of elastic wave and then unloading wave, the deformation of soft punch is just starting.

From 300 ns to 600 ns, square holes are punched on the thin metal workpiece in an extremely short interval. Initially, the shock wave propagates from the soft punch to thin metal workpiece. Due to the constraint of punching die, the workpiece is stretched around the contour of die-opening where the max Von Mises stress occurs at that moment, namely the elastic deformation stage of punching process takes place. And soon, the increasing stress climbs over the dynamic yield strength. The plastic deformation occurs along the sheared edges firstly, and then it gradually transfers to the blanking part region. When the laser energy is set as a constant, the duration of plastic deformation stage mainly depends on the workpiece's thickness. When the shear stress exceeds the dynamic fracture strength, the material's ductility losses and damage failure initiates. Compared with a general metal

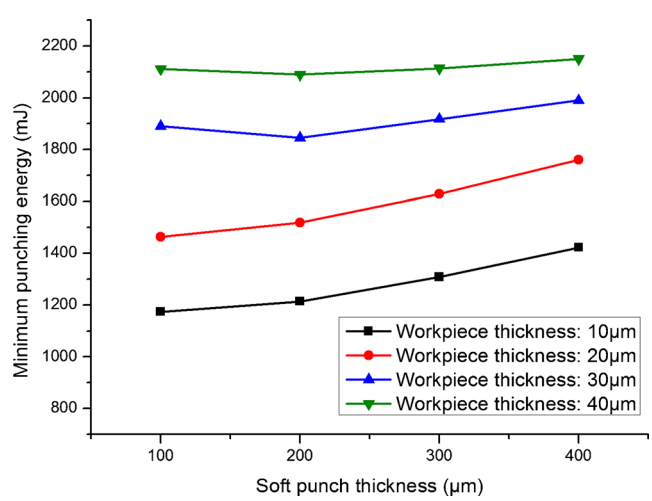

Fig. 10 For various thick workpiece, the relationship between soft punch thickness and minimum punching energy

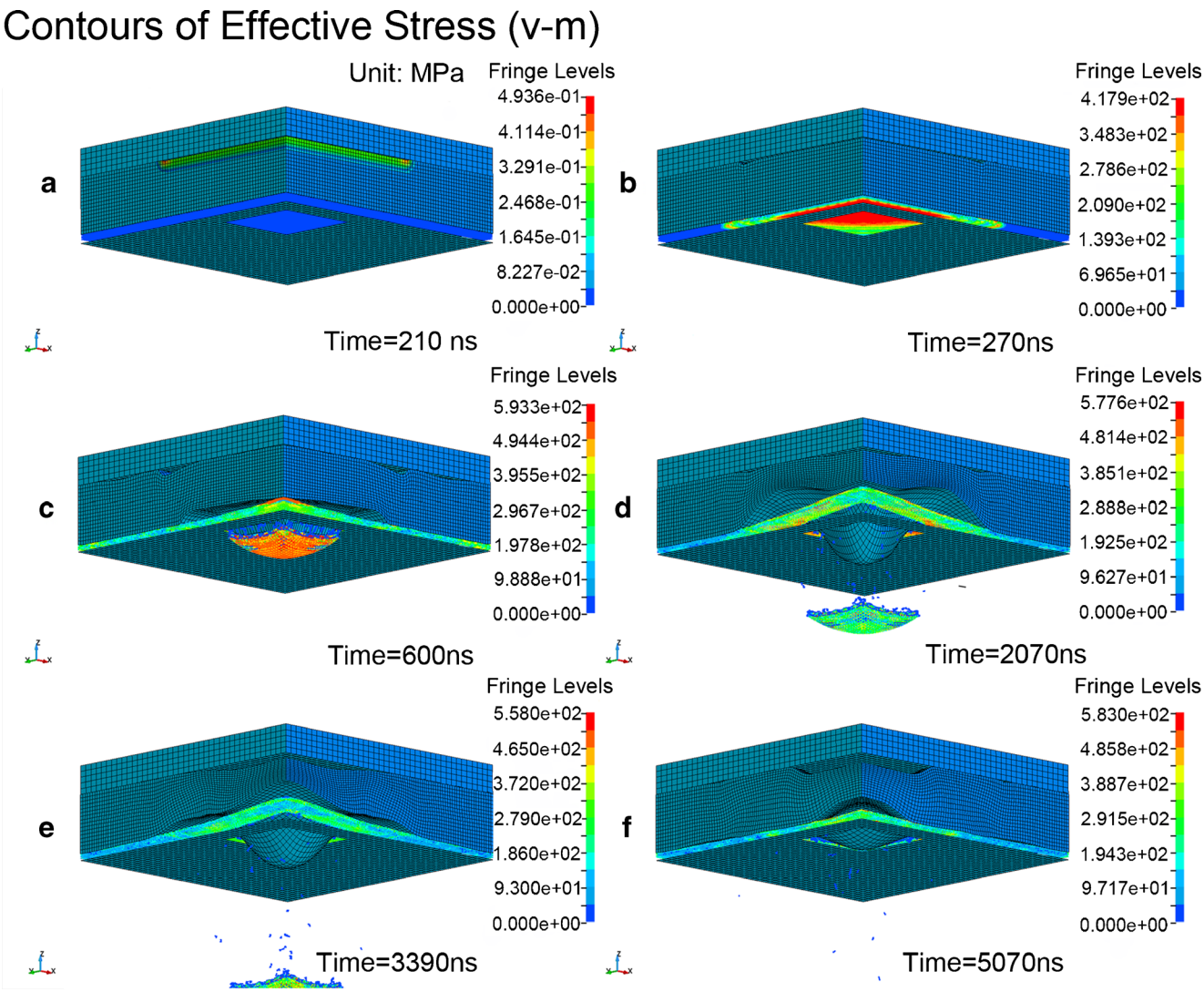

Fig. 11 The details of dynamic deformation of soft punch in the punching process, using a die model shown in Fig. 7a

punch, the soft punch has the same function in this duration, which is shown in Fig. 11c, d.

From 600 ns to 2100 ns, the rubber material of soft punch continues to flow into the die-opening for the inertial effect, thus leading to a cavity at the interface of soft punch and workpiece. Considering the size effect in the actual state that the influence of interface viscosity and friction increases in microforming process, a corresponding springback of workpiece also occurs at the meantime. At the time 2070 ns, the cavity's volume gets its maximum. The rubber material no longer flows to the die-opening, then demould stage starts.

From 2100 ns to 5200 ns, demould stage is in process. The soft punch in the shape of an asymmetric pour cone starts to spring back. It is drawn out from the die-opening and then the punched hole soon. Finally, the low surface of the soft punch restores its flatness. The process is described in Fig. 11e, f. Compared with a metal punch, the soft punch with a hyperelastic characteristic still has such advantages as demould is rather easy and the fracture surface quality is better for avoiding abrasion. The vibration occurs in the central region of soft punch's lower surface, shown in Fig. 12a. And a response vibration is also taking place in workpiece, shown in Fig. 12b. At the end of this process, the lower surface of soft punch restores its flatness. The springback of thin metal workpiece is also reduced eventually.

Effect of die-openings' scale

A contrastive study is conducted by using another die model with smaller scale die-openings, as Fig. 13 shows. It can be found that the required laser energy increases, while the duration of punching process decreases. The vibration amplitudes of soft punch and workpiece have reduced greatly. On the contrary, the frequency has increased a lot. Figure 14 reveals the Z displacement -Time curve of some specified nodes of soft punch and workpiece respectively.

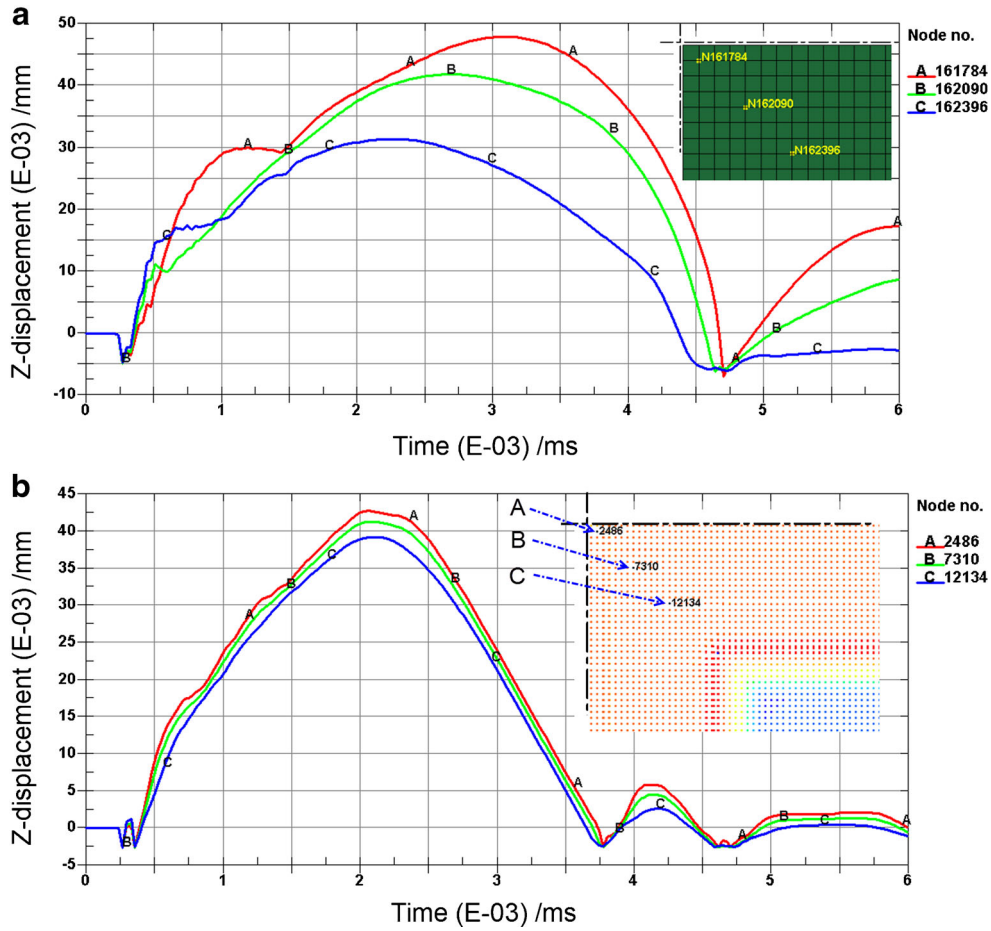

Fig. 12 The vibration behavior of soft punch and workpiece in the condition of using the die model shown in Fig. 7a: **a** The soft punch's vibration behavior shown by Z-displacement—Time curve; **b** The workpiece's response vibration behavior shown by Z displacement—Time curve

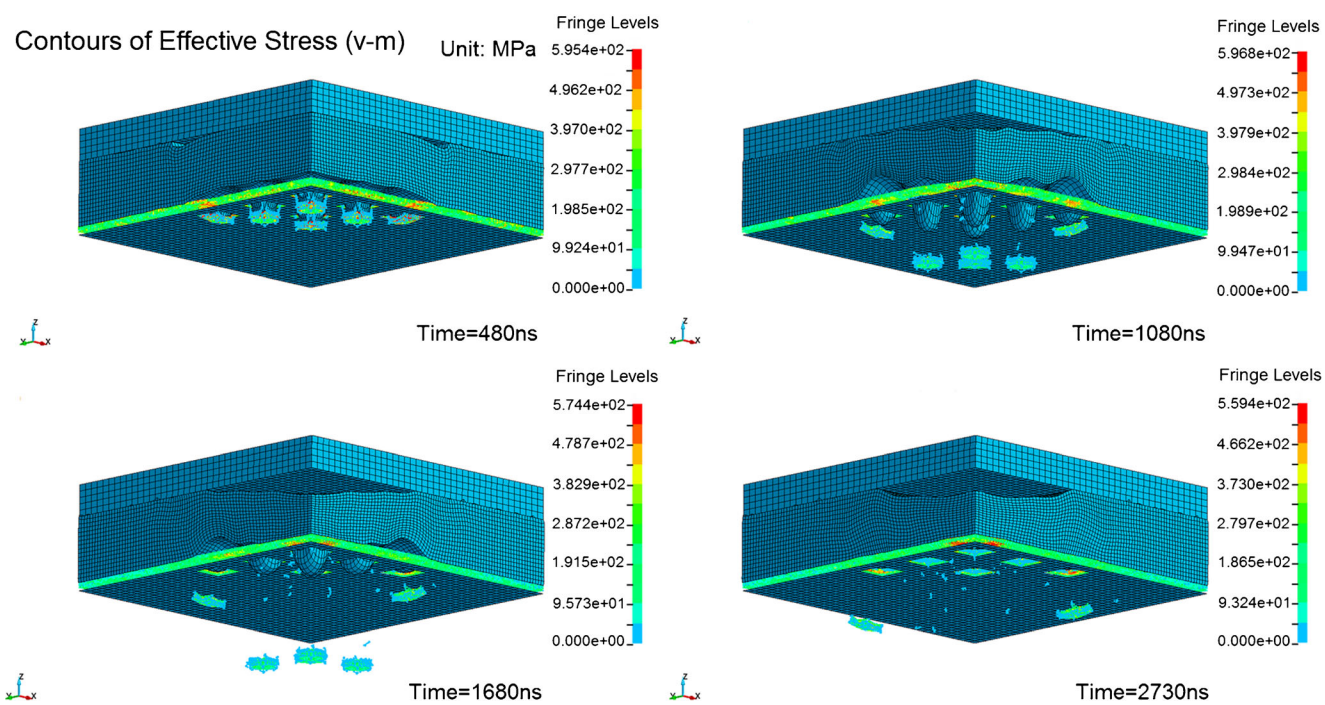

Fig. 13 The details of dynamic deformation of soft punch in the punching process, using a die model shown in Fig. 7b

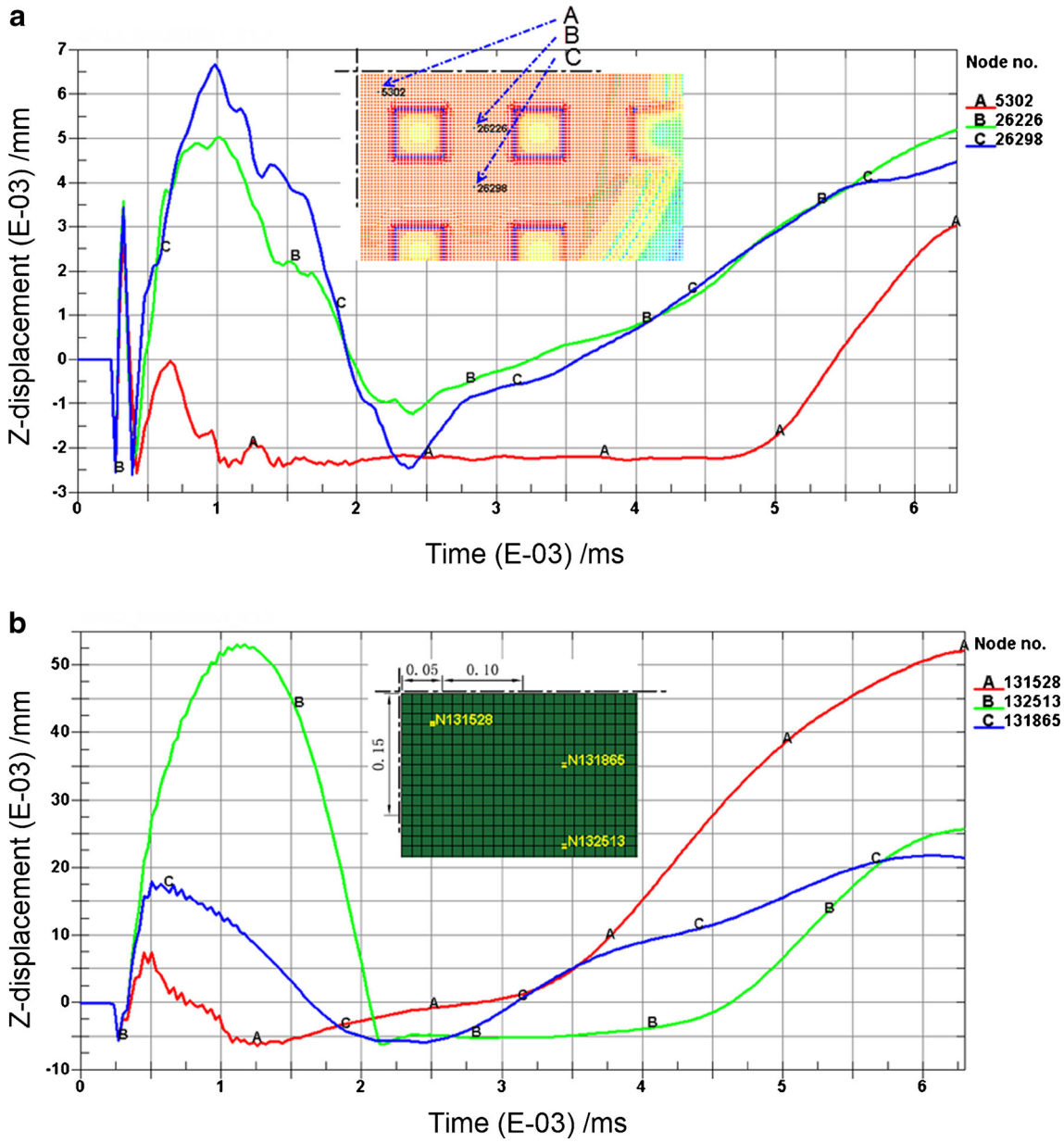

Fig. 14 The contrastive investigation of the vibration behavior of soft punch and workpiece in the condition of using the die model shown in Fig. 7b: **a** The workpiece's vibration behavior; **b** The soft punch's vibration behavior

Details in punched section and material flowing behavior

Figure 15 shows the evolution of Von Mises stress distribution in cross section at $Y=0.10$ mm. At the time 287 ns, some SPH particles on the lower surface around the contour of die-opening start to fail, namely, cracks occur in an actual state. At the time 324 ns, the fierce plastic deformation occurs in the cross section and more material flow takes place on the upper surface around the contour of die-opening, namely the thickness of punched section becomes slightly larger in Fig. 15 (Time=324 ns). At the time 324 ns, most of the particles in the punched section have failed. At the time 666 ns, punching process is completed and the springback is taking place in the central zone of the workpiece. In this picture, the material flowing is not obvious. Considering this, detailed information is given in Fig. 16. Five SPH particles in graphic position are selected. The evolution of their Y-coordinates is studied. It can be found that the maximum material flowing occurs in the middle position of sheared edges and the minimum material flowing occurs near the corners of square holes. Generally, as the thin metal workpiece is constrained by various tools and this punching is a hyperdynamic and ultrahigh strain rate

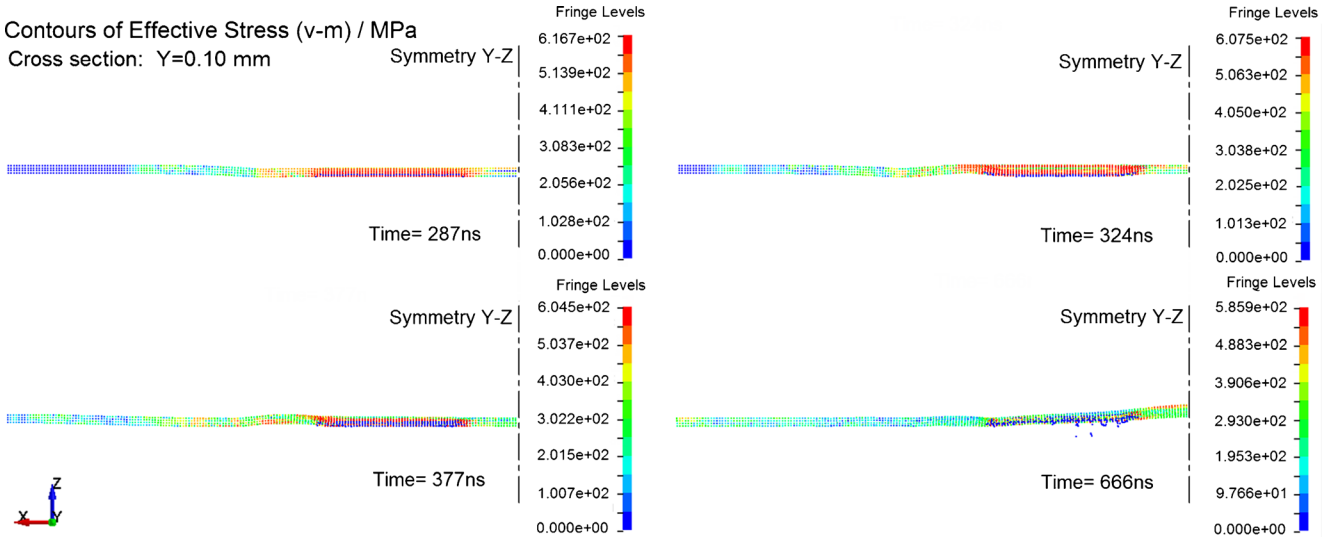

Fig. 15 The evolution of equivalent effective stress (v-m) and deformation in the cross section

process, the material flowing takes place in rather finite space and time interval. However, when the workpiece thickness increases or the laser energy decreases, the flowing area expands and flowing direction changes with a trend towards the center of blanking. Obviously, the ratio of the laser pulse energy to soft punch thickness should be an appropriate value.

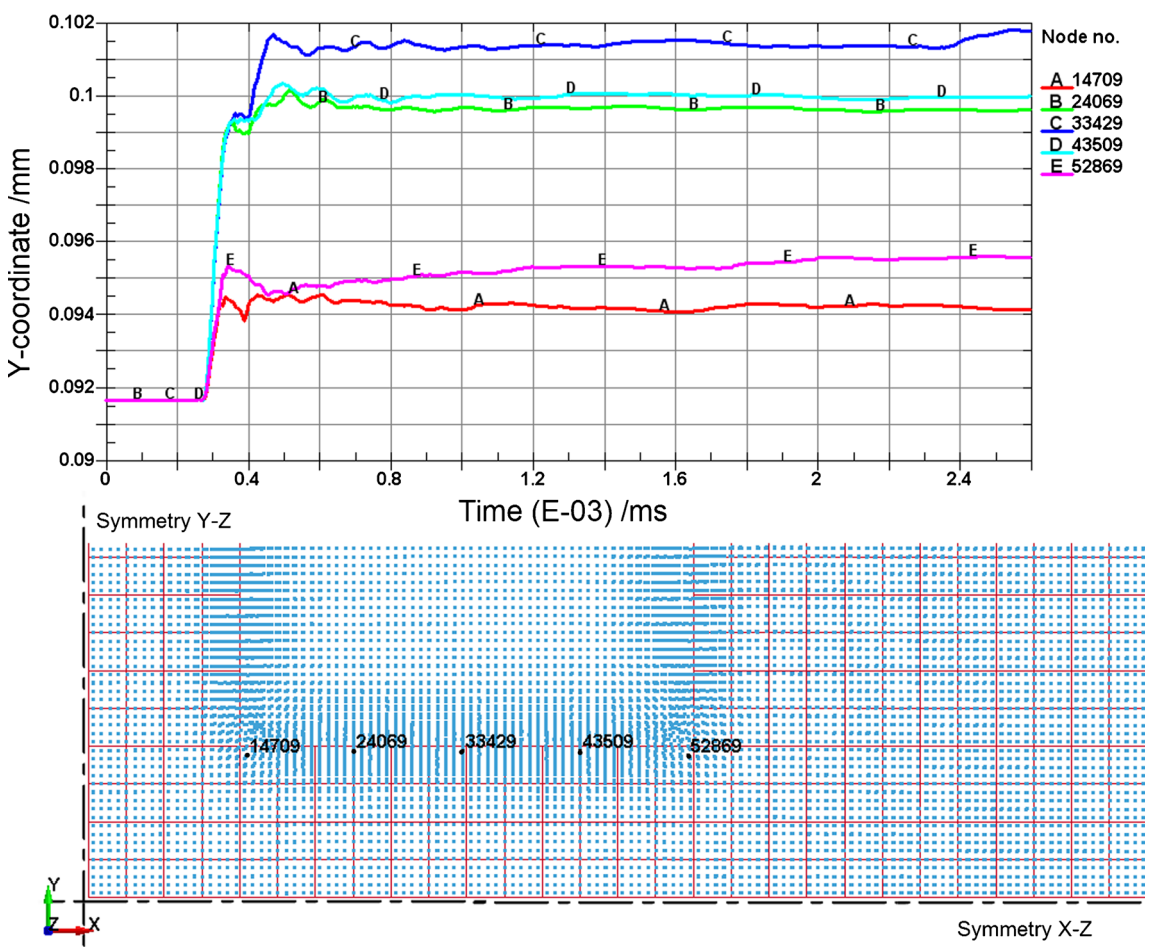

Fig. 16 The Y-coordinate—Time curve of some specified nodes, which reveals the material flowing around the sheared edge

Conclusions

This paper is intended to present a novel micro scale laser dynamic flexible punching technology in the field of thin metal sheet micro-punching. Both experiments and simulations are used to confirm reliability of this technology. In the experiments, arrays of square holes of 300 μm×300 μm in size are punched, and the quality of sheared edges is good. The polyurethane rubber working as soft punch plays a significant role in this process. The effect of key parameters such as laser energy and soft punch thickness is investigated. In the simulations, the forming mechanism of this process is investigated in detail. And the evolutions of soft punch's and workpiece's deformation are revealed. In addition, material flowing in the punching process is also studied. The results obtained are as follows:

(1) The microscale laser dynamic flexible punching is a feasible technology with advantages such as homogenizing pressure, easy demould and reducing springback.
(2) The thickness of soft punch should be selected in a proper range, and the proposed value is 100–200 μm. The ratio of the laser pulse energy to soft punch thickness should be an appropriate value, in order to obtain good punching quality. The numerical simulation turns out to be effective and prospective, and it can be used as a reference to guide the subsequent experiments.
(3) The novel technology is promising for thin metal sheet punching even in complex shapes and micro scale application. However, much work still needs to be done and more exploration is considered necessary, such as the investigation of burrs, the quality of fracture surface, and a better leveling blanking.

Acknowledgments The work is supported by the National Natural Science Foundation of China (No. 51175235), the Natural Science Foundation of Jiangsu Province (No. BK 2012712) and the Natural Science Foundation of the Jiangsu Higher Education Institutions of China (No.13KJB460003).

References

1. Joo BY, Oh SI, Jeon BH (2001) Development of micro punching system. CIRP Ann Manuf Technol 50(1):191–194. doi:10.1016/S0007-8506(07)62102-7
2. Xu J, Guo B, Shan D, Wang Z, Li M, Fei X (2013) Micro-punching process of stainless steel foil with micro-die fabricated by micro-EDM. Microsyst Technol:1–7. doi:10.1007/s00542-013-1768-1
3. Geiger M, Kleiner M, Eckstein R, Tiesler N, Engel U (2001) Microforming. CIRP Ann Manuf Technol 50(2):445–462. doi:10.1016/S0007-8506(07)62991-6
4. Masuzawa T, Fujino M, Kobayashi K, Suzuki T, Kinoshita N (1985) Wire electro-discharge grinding for micro-machining. CIRP Ann Manuf Technol 34(1):431–434. doi:10.1016/S0007-8506(07)61805-8
5. Chern G-L, Wu Y-JE, Liu S-F (2006) Development of a micro-punching machine and study on the influence of vibration machining in micro-EDM. J Mater Process Technol 180(1–3):102–109. doi:10.1016/j.jmatprotec.2006.05.010
6. Qin Y, Ma Y, Harrison C, Brockett A, Zhou M, Zhao J, Law F, Razali A, Smith R, Eguia J (2008) Development of a new machine system for the forming of micro-sheet-products. Int J Mater Form 1(1):475–478. doi:10.1007/s12289-008-0098-9
7. Santo L, Quadrini F, Trovalusci F (2010) A miniaturized machhine for micro-sheet forming. Int J Mater Form 3(1):1091–1094. doi:10.1007/s12289-010-0961-3
8. Xu J, Guo B, Shan D, Wang C, Li J, Liu Y, Qu D (2012) Development of a micro-forming system for micro-punching process of micro-hole arrays in brass foil. J Mater Process Technol 212(11):2238–2246. doi:10.1016/j.jmatprotec.2012.06.020
9. Joo B-Y, Rhim S-H, Oh S-I (2005) Micro-hole fabrication by mechanical punching process. J Mater Process Technol 170(3):593–601. doi:10.1016/j.jmatprotec.2005.06.038
10. Presz W (2008) Contact phenomena in micro-blanking. Int J Mater Form 1(1):471–474. doi:10.1007/s12289-008-0097-x
11. Watari H, Ona H, Yoshida Y (2003) Flexible punching method using an elastic tool instead of a metal punch. J Mater Process Technol 137(1–3):151–155. doi:10.1016/S0924-0136(02)01080-4
12. Rhim SH, Son YK, Oh SI (2005) Punching of ultra small size hole array. CIRP Ann Manuf Technol 54(1):261–264. doi:10.1016/S0007-8506(07)60098-5
13. Zhou JZ, Yang JC, Zhang YK, Zhou M (2002) A study on super-speed forming of metal sheet by laser shock waves. J Mater Process Technol 129(1–3):241–244. doi:10.1016/S0924-0136(02)00609-X
14. Liu H, Shen Z, Wang X, Wang H, Tao M (2010) Numerical simulation and experimentation of a novel micro scale laser high speed punching. Int J Mach Tools Manuf 50(5):491–494. doi:10.1016/j.ijmachtools.2010.02.003
15. Liu H, Wang H, Shen Z, Huang Z, Li W, Zheng Y, Wang X (2012) The research on micro-punching by laser-driven flyer. Int J Mach Tools Manuf 54–55:18–24. doi:10.1016/j.ijmachtools.2011.12.004
16. Handbook ASM (1988) Forming and forging. ASM Int 14:483
17. Sung-Lim K, Dornfeld DA (1996) Analysis of fracture in burr formation at the exit stage of metal cutting. J Mater Process Technol 58(2–3):189–200. doi:10.1016/0924-0136(95)02124-8
18. Wang X, Du D, Zhang H, Shen Z, Liu H, Zhou J, Liu H, Hu Y, Gu C (2013) Investigation of microscale laser dynamic flexible forming process—simulation and experiments. Int J Mach Tools Manuf 67:8–17. doi:10.1016/j.ijmachtools.2012.12.003
19. Hallquist JO (2006) LS-DYNA theory manual. Livermore Softw Technol Corp 3
20. Johnson GR, Cook WH (1983) A constitutive model and data for metals subjected to large strains, high strain rates and high temperatures. International Ballistics Committee, The Hague, pp 541–547
21. Johnson GR, Cook WH (1985) Fracture characteristics of three metals subjected to various strains, strain rates, temperatures and pressures. Eng Fract Mech 21(1):31–48. doi:10.1016/0013-7944(85)90052-9
22. Kay G (2002) Failure modeling of titanium-61-4 V and 2024-T3 aluminum with the Johnson-Cook material model. Technical Rep, Lawrence Livermore National Laboratory, Livermore
23. Dirikolu MH, Akdemir E (2004) Computer aided modelling of flexible forming process. J Mater Process Technol 148(3):376–381. doi:10.1016/j.jmatprotec.2004.02.049
24. Fabbro R, Fournier J, Ballard P, Devaux D, Virmont J (1990) Physical study of laser-produced plasma in confined geometry. J Appl Phys 68(2):775–784. doi:10.1063/1.346783
25. Peyre P, Fabbro R (1995) Laser shock processing: a review of the physics and applications. Opt Quant Electron 27(12):1213–1229